JOURNAL OF MATERIALS SCIENCE 31 (1996) 1221–1229

Effect of load on tribological behaviour of carbon–carbon composites

J. D. CHEN, J. H. CHERN LIN, C. P. JU
Department of Materials Science and Engineering, National Cheng-Kung University, Tainan, Taiwan

The effect of load on the tribological behaviour of three different two-dimensional carbon–carbon composites, including polyacrylonitrile (PAN) fibre-pitch matrix, PAN fibre-chemical vapour infiltrated (CVI) matrix, and pitch fibre-resin/CVI hybrid matrix composites has been compared. Results indicated that friction and wear rate variations with slide distance depended on load and the type of composite. The worn surface morphology was categorized into three types (I, II and III). The friction coefficient, wear rate and temperature all increased sharply when the transition from type I to type II occurred. When the powdery type II debris was compacted to form the lubricative type III debris, the friction coefficient and wear rate declined, although never approached their initial type I levels. For all composites, a higher load can accelerate the transition from type I to type II, but impedes the transition from type II to type III. Under 2.4 MPa, the type II morphology was never observed to transform into type III morphology in this study.

1. Introduction

Owing to their low density, excellent thermal and mechanical properties, self-lubricating and low-wear capability, carbon–carbon (C–C) composites have emerged as a strong aircraft brake (rotator and stator) material [1–3]. Compared to conventional steel/ceramet brakes, C–C composites apparently performed better in weight saving and brake life [1].

The C–C composites currently used as aircraft brake discs are either PAN/CVI-based or pitch/resin/CVI-based composites. Owing to their different formulae and processes, the friction and wear performance of the different composites was different. Recently, the friction and wear performance of a series of two-dimensional PAN/pitch composites has been evaluated under low and medium-energy conditions [4–7]. The preliminary results indicated that the PAN/pitch composite might also be promising for use as brake material.

Friction and wear behaviour of a C–C brake disc depends upon many parameters, such as fibre and matrix types, load, speed, temperature and humidity, to name a few. Although the effects of speed, humidity and surface morphology have been studied in our laboratories and elsewhere [3–10], the effect of load on the friction and wear behaviour of C–C has been little discussed in the open literature. Clark *et al.* [11] and Tanvir [12] found that, for a bulk carbon/graphite sliding against the self material, an increase in load resulted in a decrease in friction. Quinn [13] and Fusaro [14] showed that, for either a bulk carbon/graphite or carbon fibre-reinforced resin composite sliding against metals, the higher load yielded a lower friction coefficient.

The present work compared the effect of load on the tribological behaviour of three different two-dimensional C–C composites, including polyacrylonitrile (PAN) fibre-pitch matrix, PAN fibre-chemical vapour infiltrated (CVI) matrix, and pitch fibre-resin/CVI hybrid matrix composites. It should be noted that the relative slide speeds used in the present study were only in the realm of the "taxi" condition of aircraft due to the large difference in disc diameter.

2. Experimental procedure

As shown in Table I, the three C–C composites used in this study had different fibre and/or matrix, and were fabricated by different techniques. The two-dimensional PAN/CVI (designated E) composite was fabricated from stacked dry PAN-based fibre laminates which were infiltrated/densified by CVI. The two-dimensional pitch/resin/CVI (designated A) hybrid matrix composite was fabricated from carbonized mesophase pitch fibre-phenolic resin prepregs which were subsequently densified by CVI. The two-dimensional PAN/pitch (designated TM) composite was fabricated using woven high-modulus PAN-based fibre preforms which were pressure-infiltrated and densified with molten matrix pitch. The detailed processing of this composite has been described elsewhere [15].

A fixed rotor speed of 2000 r.p.m., equivalent to an average linear speed of 1.832 m s^{-1}, and three different loads (1.0, 1.7 and 2.4 MPa) were used in this study. The C–C discs had a radius of 0.875 cm, and each cycle was equivalent to an average linear slide distance of 5.5 cm. Prior to testing, all specimens were mechanically polished through a level of 1200 grit paper,

0022–2461

TABLE I Carbon–carbon composites tested in this study

	E	TM	A
Weave pattern/yarn size	Laminated mat/1 K	8H-satin/2 K	Chopped 8H/satin/4 K
Formula	PAN/CVI	PAN/pitch	Pitch/resin/CVI
Dimensionality	2	2	2
Flexural strength (MPa)	92	120	53
Density ($g\,cm^{-3}$)	1.76	1.72	1.74

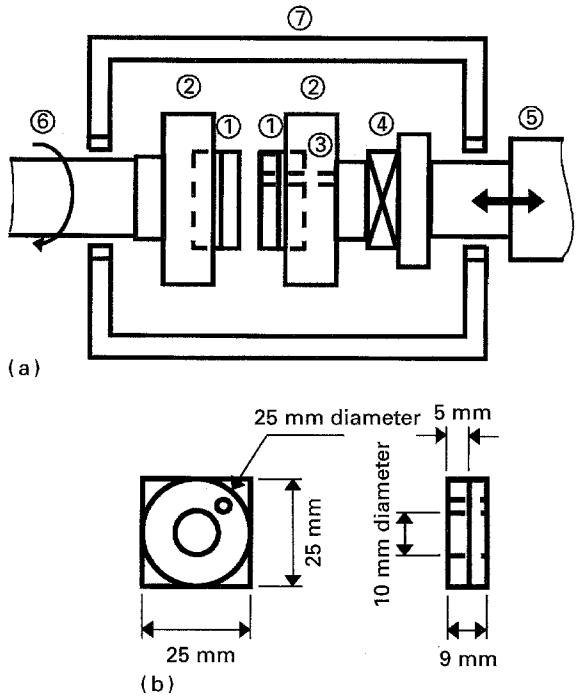

Figure 1 Schematic drawing of (a) the wear tester and (b) the specimen. (a) 1, specimen; 2, specimen holder; 3, thermocouple; 4, dynamometer; 5, loading system; 6, rotating shaft; 7, specimen chamber.

followed by ultrasonic cleaning and drying. The sliding torques, which were used to calculate friction coefficients, were recorded *in situ* using an AST-BH dynamometer (Sato, Japan). Each weight loss value was an average of four fresh runs. Because the rotor and the stator were always of identical material, the weight losses from both discs were measured and their average values were taken. An FM2 camera (Nikon, Japan) and ABT-55 scanning electron microscope (SEM) (Topcon, Japan) was used to examine as-polished and worn surfaces of each composite.

The temperature induced in the friction and wear processes was measured using a chromel–alumel type thermocouple which, through a 3 mm diameter graphite tube, was inserted from the back (non-sliding side) of stator to a position of approximately 1 mm beneath the slide surface (Fig. 1). It should be noted that "true" temperatures at the very contact surfaces must be higher than the measured ones.

3. Results

3.1. Friction

Typical curves of variation in friction coefficient with slide distance for the three different composites slid at

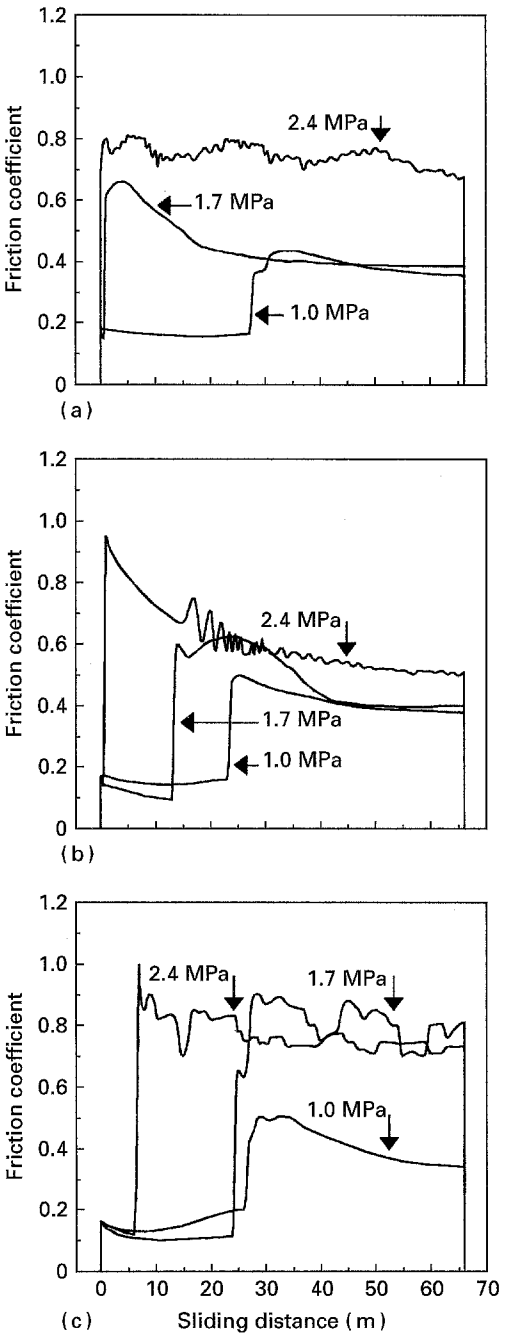

Figure 2 Friction coefficient variation with sliding distance at 2000 r.p.m. in air. (a) E, (b) TM, (c) A.

2000 r.p.m. under three different loads (1.0, 1.7 and 2.4 MPa) are shown in Fig. 2 (note: more than four tests have been run under each condition and the curves shown in Fig. 2 are the very typical ones). As shown in the figure, all three composites slid under a load of 1.0 MPa exhibited low friction coefficient (0.1–0.2) in the first 20 m or so. After this low-friction

period, a transition occurred to all composites accompanying an abrupt rise in friction coefficient (to 0.4–0.5, depending on the composite), then decreased with time to steady values (about 0.35 for composites E and A and 0.4 for the composite TM).

Under the load of 1.7 MPa, composite E did not show a transition in friction coefficient. After the initial peak, the friction coefficient declined to a quite steady value of 0.4 at the conclusion of the test (66 m). The transitions which occurred in composites TM and A were easily identified. For the composite TM, the transition took place after about 13 m sliding and, after that, the friction coefficient decreased from its peak value of 0.6 to a steady value of about 0.4. For composite A, the transition occurred at about 25 m. Quite differently from the other two composites slid under the same load, the post-transitional friction coefficient of composite A did not significantly decrease. Rather, it had maintained a high level of 0.7–0.9.

When the composites were slid under 2.4 MPa, transition was observed in neither composite En or TM. For composite A, however, the transition was easily identified but occurred much earlier (at about 6 m) than that under 1.7 or 1.0 MPa (in the neighbourhood of 25 m). After the initial peak (0.95), the friction coefficient of composite TM decreased to 0.5 at 66 m. For composites E and A, however, the friction coefficients stayed high (0.7–0.9) after the initial peaks. The friction coefficient curves of the composite A were the most rugged of the three composites under high loads.

3.2. Wear

Fig. 3 shows the wear rates (weight loss/area/sliding distance) of the three composites (E, TM and A) under different loads (1.0, 1.7 and 2.4 MPa) at different slide distances (3.3, 16.5, 33 and 66 m). In general, the wear rates increased with increasing load when the other parameters were fixed. For comparison with some data in the literature, the wear rates in terms of weight losses per unit energy (or weight loss/area/sliding distance/load) are shown in Fig. 4.

Under the load of 1.0 MPa, all three composites had a similar trend in wear-rate variation with slide distance. The wear rates dropped initially from 6×10^{-5} mg N^{-1} m^{-1} (3.3 m) to 1.9×10^{-5} mg N^{-1} m^{-1} (16.5 m) for the composite E; from 7×10^{-5} mg N^{-1} m^{-1} to 2.2×10^{-5} mg $N^{-1}m^{-1}$ for TM, and from 5×10^{-5} mg N^{-1} m^{-1} to 1.8×10^{-5} mg N^{-1} m^{-1} for A. Figs 3 and 4 clearly indicated that a transition in wear rate had occurred to all composites somewhere between 16.5 and 33 m. When the transition occurred, the wear rates of the composites sharply increased by about an order of magnitude, then graduately declined. At the conclusion of the test (66 m), the composite TM had the largest wear rate value (35×10^{-5} mg N^{-1} m^{-1}), while E had the smallest value (12×10^{-5} mg N^{-1} m^{-1}).

When slid under 1.7 MPa, the three composites behaved quite differently. The transition occurred to the composite A between 16.5 and 33 m; to TM, between 3.3 and 16.5 m; and, to E, too early to be

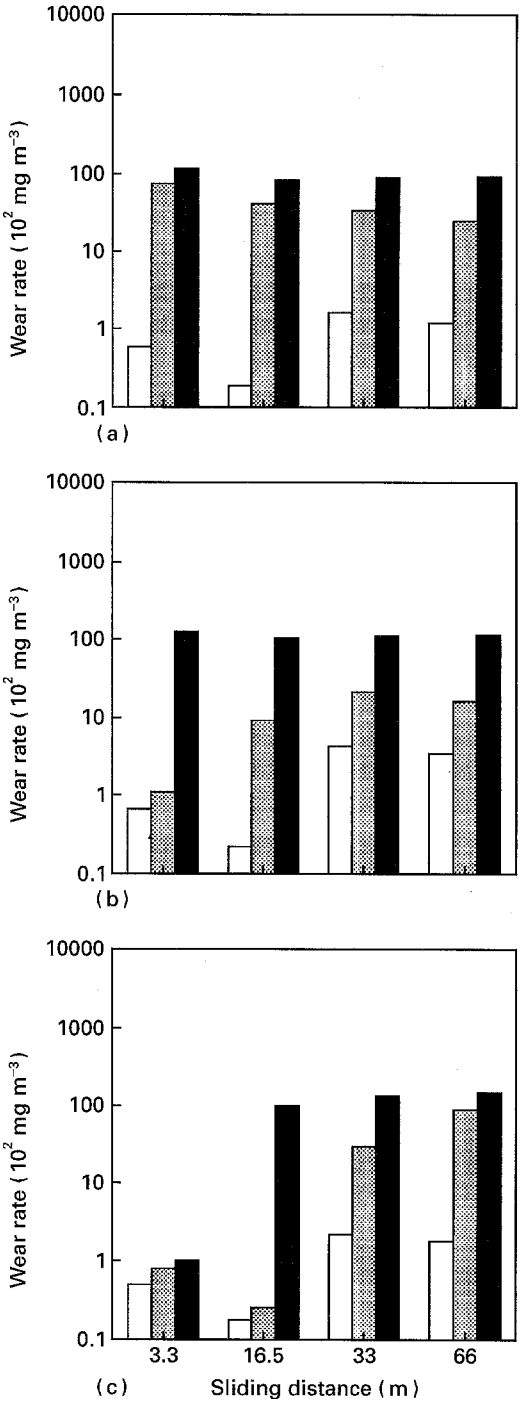

Figure 3 Wear-rate (weight loss/area/sliding distance) variation with sliding distance at 2000 r.p.m. in air. (a) E, (b) TM, (c) A. (□) 1.0 MPa, (▨) 1.7 MPa, (■) 2.4 MPa.

identified. Again, the occurrence of the transitions in wear were consistent with the occurrence of the transitions in friction. After the initial peak value (445×10^{-5} mg N^{-1} m^{-1}), the wear rate of E gradually went down (to 144×10^{-5} mg N^{-1} m^{-1} at 66 m). The post-transitional wear rate of TM continued to increase to 129×10^{-5} mg N^{-1} m^{-1} at 33 m (note the post-transitional broad peak in friction coefficient in Fig. 2), then decreased to 98×10^{-5} mg N^{-1} m^{-1} at 66 m. Rather than going down, the post-transitional wear rate of A further increased to 529×10^{-5} mg N^{-1} m^{-1} at 66 m. This corresponded to the non-decreasing post-transitional friction coefficient (Fig. 2) of this composite. At the conclusion of

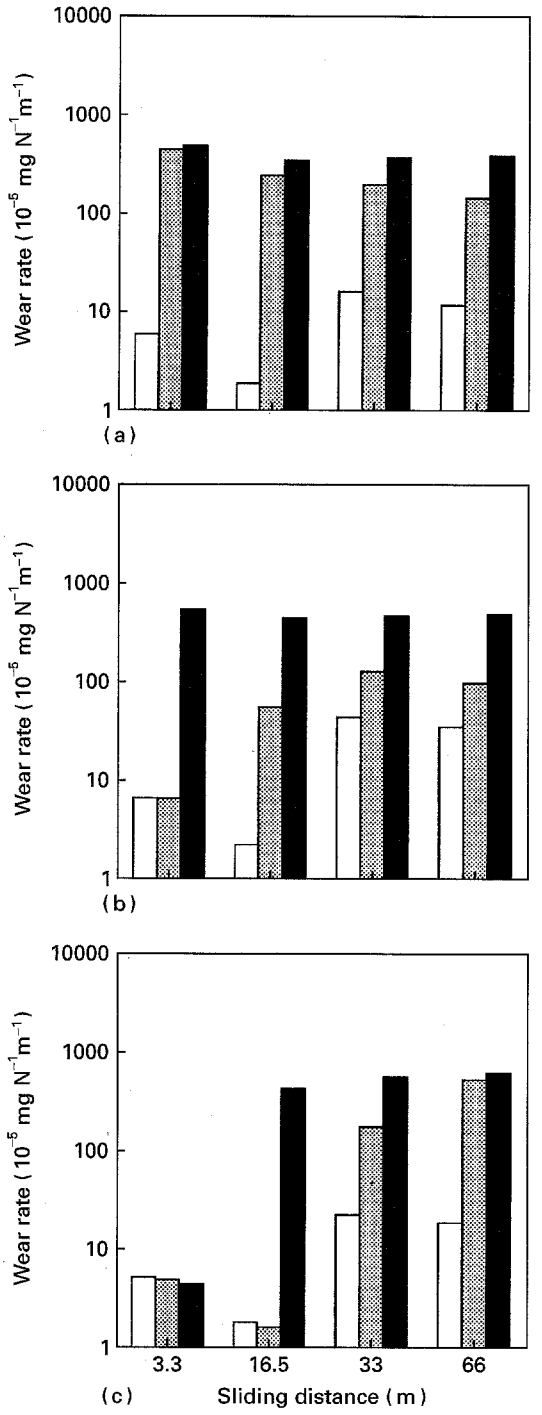

Figure 4 Wear-rate (weight loss/area/sliding distance/load) variation with sliding distance at 2000 r.p.m. in air. (a) E, (b) TM, (c) A. (□) 1.0 MPa, (▨) 1.7 MPa, (■) 2.4 MPa.

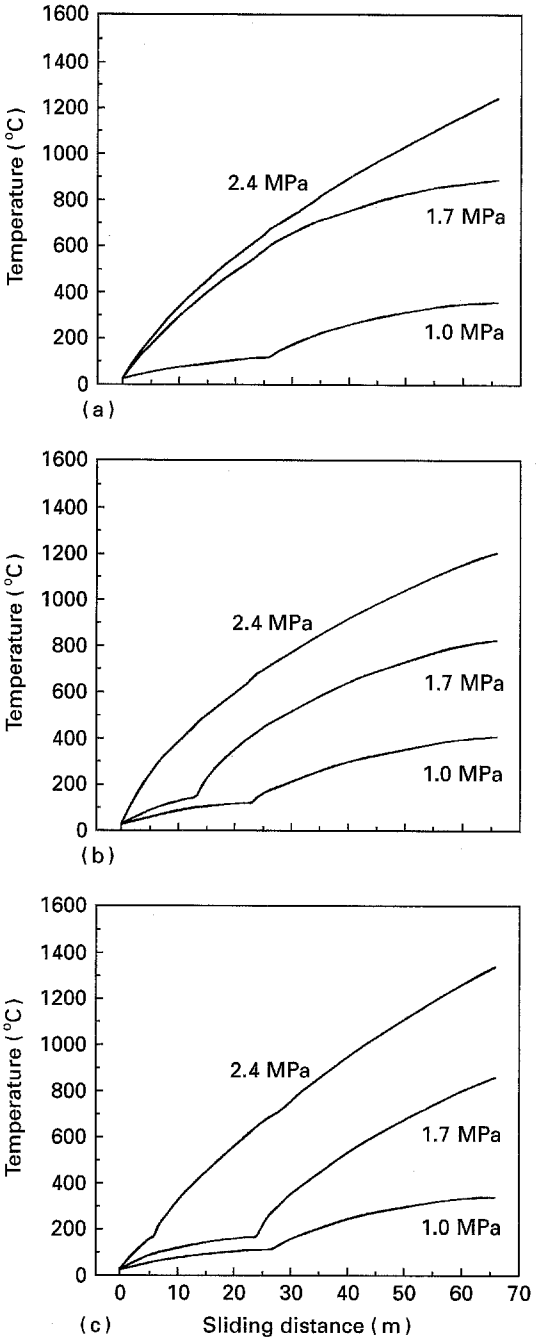

Figure 5 Temperature variation with sliding distance at 2000 r.p.m. in air. (a) E, (b) TM, (c) A.

the test, composite TM had the smallest wear rate value, while composite A had the largest of the three composites.

Under 2.4 MPa, composite A showed a transition between 3.3 and 16.5 m. Prior to the transition, the wear rate was low (4×10^{-5} mg N^{-1} m^{-1}). After the transition, the wear rate abruptly increased to 426×10^{-5} mg N^{-1} m^{-1} and then maintained a quite steady value. For composites E and TM, the wear rates were constantly high. At 66 m, composite A had a larger wear rate (622×10^{-5} mg N^{-1} m^{-1}) than those of E (390×10^{-5} mg N^{-1} m^{-1}) and TM (497×10^{-5} mg N^{-1} m^{-1}).

3.3. Temperature

The measured temperature variations with slide distance of the three composites slid under three different loads are shown in Fig. 5. As indicated in this figure, the higher the load applied, the higher the temperature which was induced. At the conclusion of the tests (66 m), the measured temperatures under the loads of 1.0, 1.7 and 2.4 MPa were, respectively, 360, 890 and 1240 °C for composite E, 410, 830 and 1210 °C for composite TM, and 340, 860 and 1340 °C for composite A.

Under certain conditions, the slide-induced temperature rise exhibited a transition. When the transition occurred, the temperature rose more rapidly than that prior to the transition. Compared to the friction coefficient data (Fig. 2), it was found that the moments

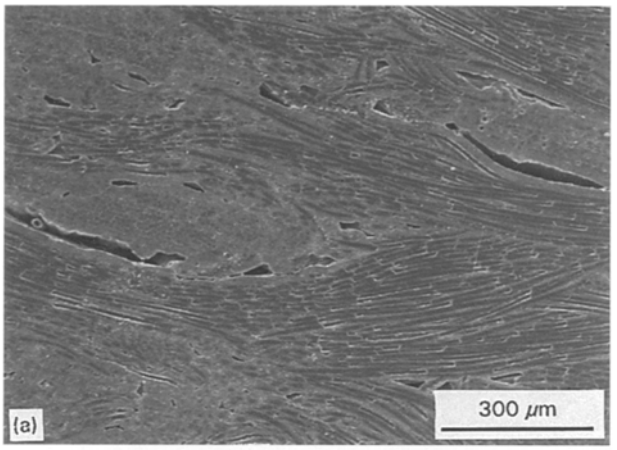

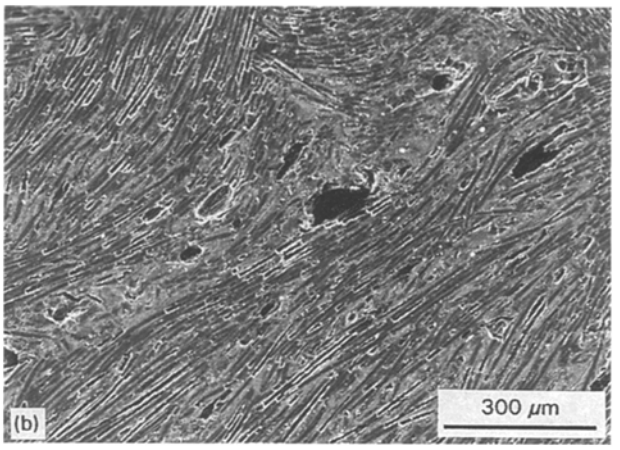

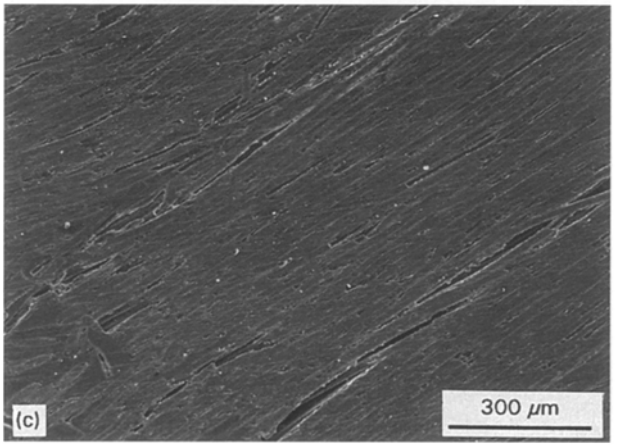

Figure 6 Scanning electron micrographs of as-polished composites: (a) E, (b) TM, (c) A.

when the transitions in friction occurred were exactly the same as when the transitions in temperature occurred.

3.4. Morphological variation

3.4.1. As-polished morphology

Composite E was comprised of woven high-modulus PAN-based fibre yarns and CVI carbon matrix (Fig. 6). Large pores (up to hundreds of micrometers long and tens of micrometres wide) were observed to locate primarily at the junctions between fibre yarns and CVI carbon. Polarized light microscopy showed that the CVI carbon was highly anisotropic, with basal planes parallel to the fibres. In composite A the mesophase fibre yarns were bonded by phenolic resin char. The thin CVI layers were not resolved in this low-magnification micrograph. Composite A was less porous than composite E (the porosity volume fractions of composites A and E were 7% and 11.1%, respectively) but had a similar density due to the presence of lower density resin char. Pores in composite A were observed either within matrix resin char or at the fibre–matrix interface.

In composite TM (Fig. 6), high-modulus PAN-based fibres were bonded by pyrolysed pitch matrix which had been pressure-infiltrated into the composite interior prior to each carbonization treatment. Polarized light microscopy indicated that the matrix pitch was anisotropic, with basal planes parallel to the fibre surface. Both open porosity volume fraction (8.5%) and pore size (several tens of micrometers being the maximum) were between those of composites E and A.

3.4.2. Worn surface morphology

Photographs of worn surfaces of the three composites slid under the three different loads (1.0, 1.7 and 2.4 MPa) at a speed of 2000 r.p.m. are shown in Fig. 7. According to the optical and SEM observation of this study, the worn surface morphology was categorized into three types (types I, II and III) and the results are summarized in Table II. Although SEM has been performed on all composites at a series of slide stages, to save space, only the typical morphologies of each type are shown (Figs 8–10).

The type I morphology, generally observed on mildly worn composite (such as those slid for short distances under 1.0 MPa) surfaces, was characterized as a thin, smooth, and bright (under light) debris film. The original as-polished structure underneath the debris film was still somewhat recognizable. The small pores observed in the as-polished structure were no longer observed, but the larger pores were still there. The type II morphology (such as those slid under 2.4 MPa), often observed on composites in which a friction and wear transition occurred, featured a thick, rough, and dark (under light) powdery debris layer. The formation of this powdery debris layer and its effect on wear has been discussed earlier [4–7]. The type III morphology (such as those slid for 66 m under 1.0 MPa), usually observed on composites slid for a while after transition, was identified as a smooth, dense, and bright (under light) debris film. This type of debris film was thicker and more stable than the type I debris film. Almost all the pores were readily filled with debris and the original structure was no longer recognizable.

4. Discussion

As shown in Fig. 2, all three composites slid under a load of 1.0 MPa exhibited a low friction coefficient (0.1–0.2) in the first 20 m or so. After this low-friction

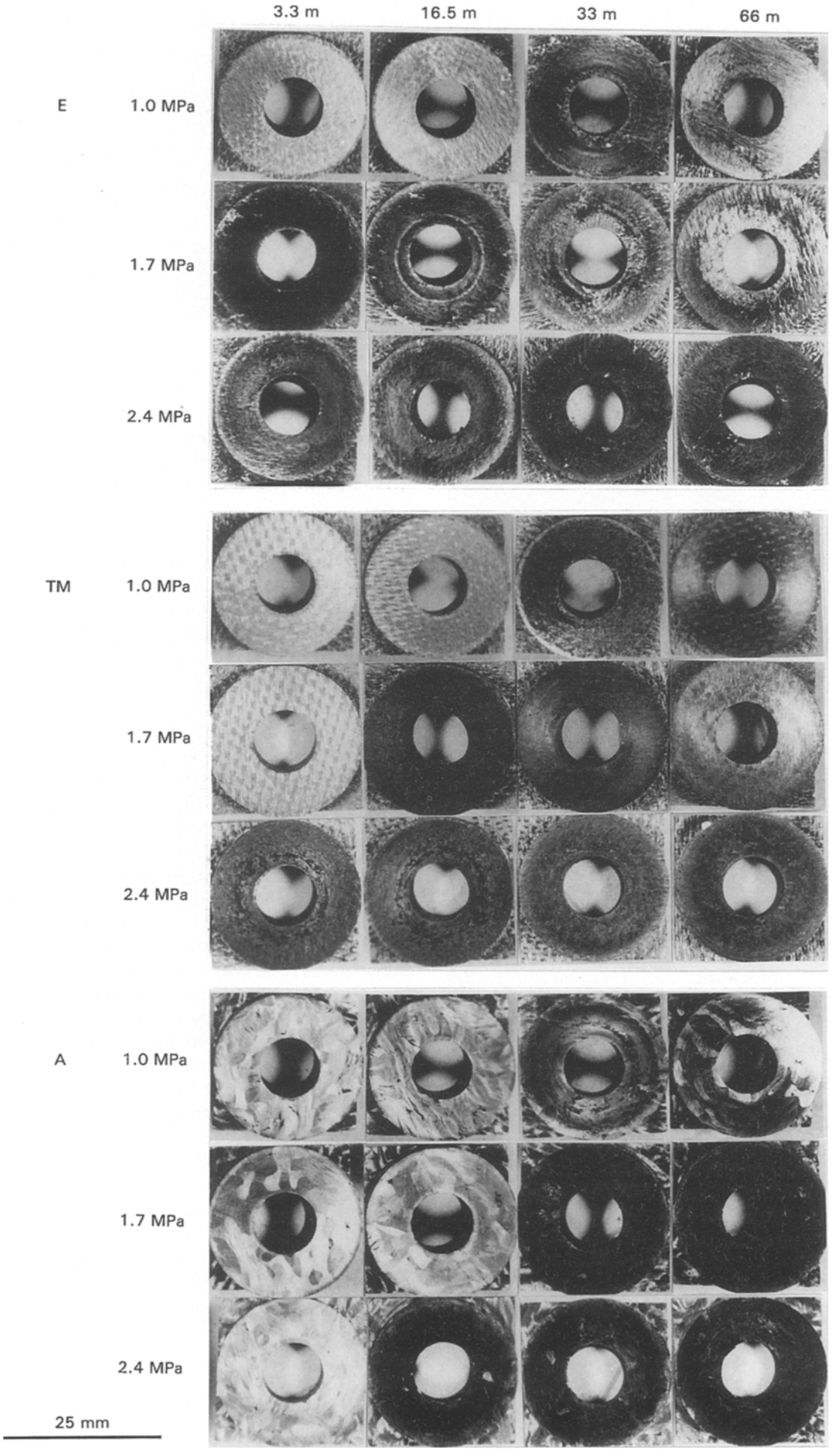

Figure 7 Photographs of worn surfaces of different composites.

TABLE II Summary of worn surface morphological variation

Material	Load (MPa)	Sliding distance (m)			
		3.3	16.5	33	66
E	1.0	○	○	◓	◍
	1.7	●	●	◓	◓
	2.4	●	●	●	●
TM	1.0	○	○	●	◍
	1.7	○	●	●	◍
	2.4	●	●	●	●
A	1.0	○	○	●	◍
	1.7	○	○	●	●
	2.4	○	●	●	●

○ Type I ● Type II
◍ Type III ◓ II + III mixed

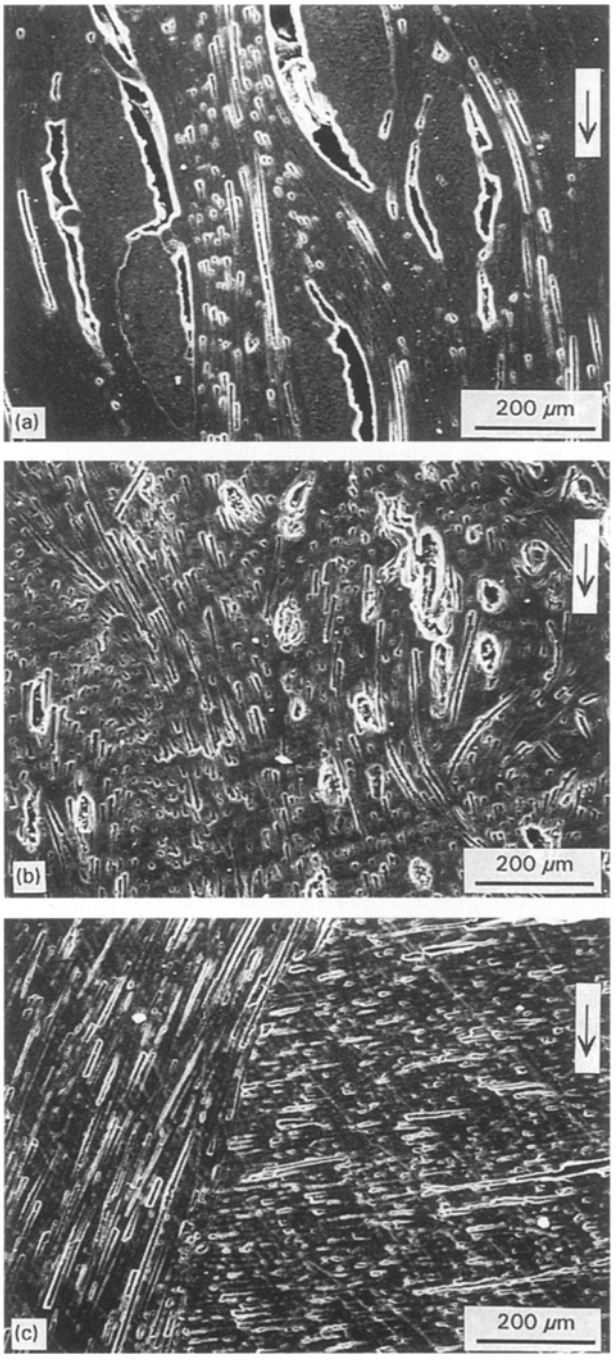

Figure 8 Scanning electron micrographs of typical type I worn surfaces (the arrow indicates the sliding direction). 1 MPa, 16.5 m. (a) E, (b) TM, (c) A.

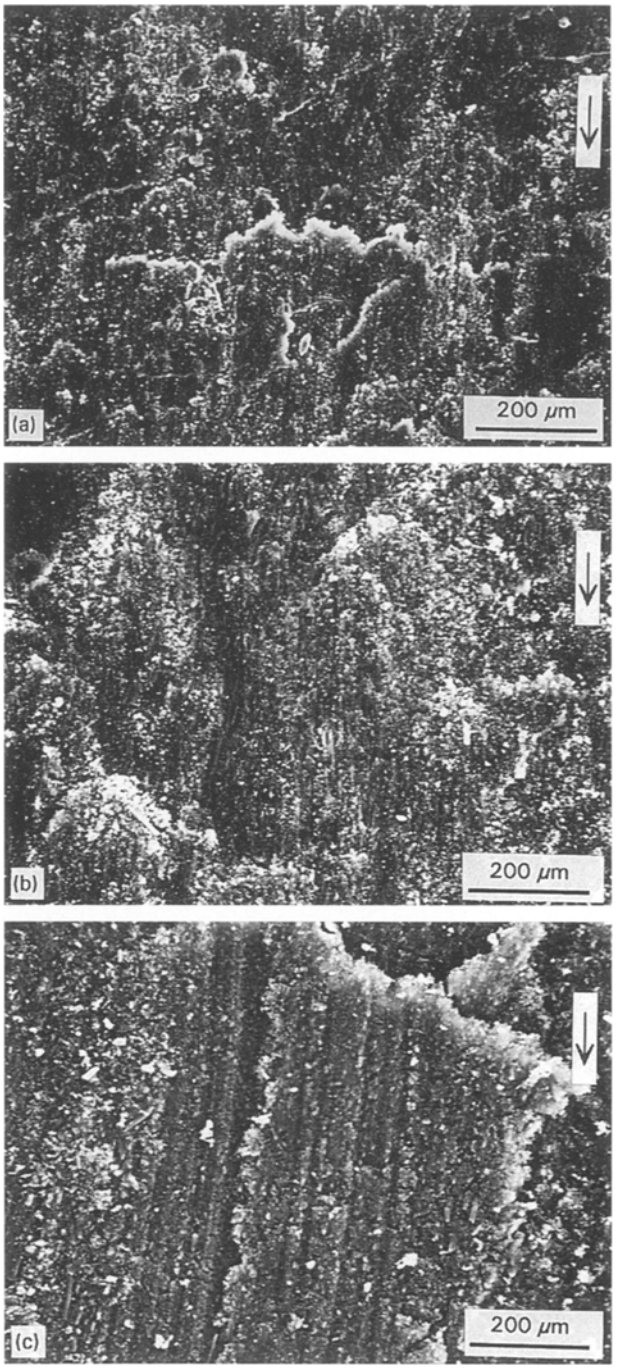

Figure 9 Scanning electron micrographs of typical type II worn surfaces (the arrow indicates the sliding direction). 1.7 MPa. (a) E (3.3 m), (b) TM (16.5 m), (c) A (66 m).

period, a transition occurred to all composites accompanying an abrupt rise in friction coefficient (to 0.4–0.5, depending on the composite), which then decreased with time to steady values. Under 1.7 MPa, composite E did not show a transition in friction coefficient. It is very likely that the transition took place too quickly to be picked up by the plotter, considering its high initial peak friction coefficient value (about 0.65). The transitions which occurred in composites TM and A were easily identified. For composite A, the post-transitional friction coefficient maintained a high level of 0.7–0.9. Under 2.4 MPa, the transition was observed in neither composite E nor TM, probably for the same reason mentioned earlier. For composite A, the transition was easily identified

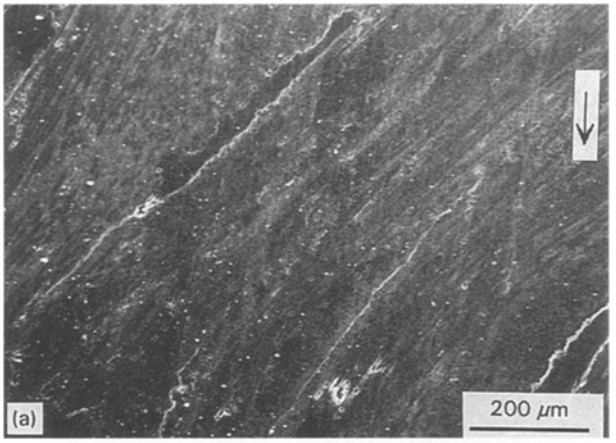

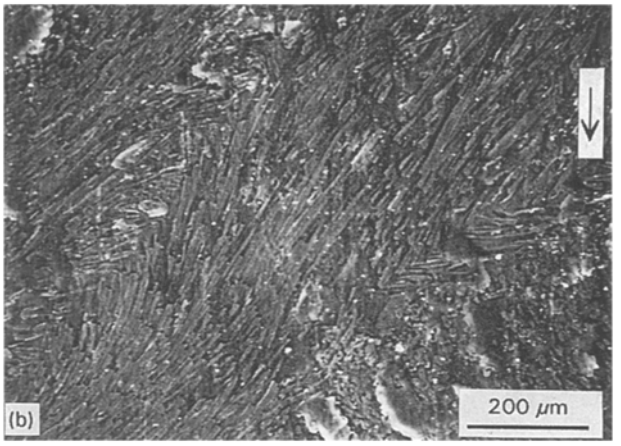

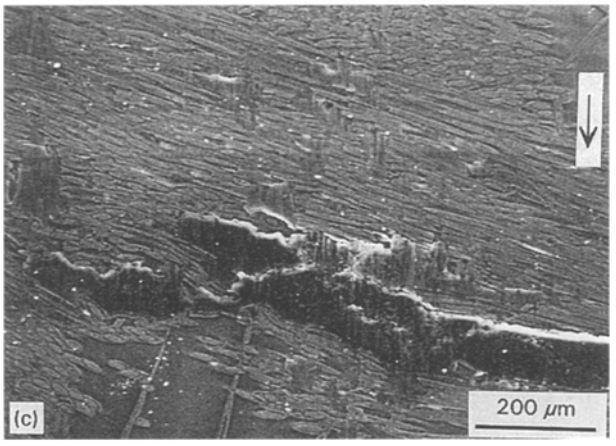

Figure 10 Scanning electron micrographs of typical type III worn surfaces (the arrow indicates the sliding direction). 1.0 MPa, 66 m. (a) E, (b) TM, (c) A.

but occurred much earlier (at about 6 m) than that under 1.7 or 1.0 MPa.

Although the weight loss always increased with slide distance for all composites, the wear rate variation with slide distance depended much on load and the type of composite. It should be noted that, because the weight losses were not recorded in a continuous manner, the moments of transitions in wear, indicated in Figs 3 and 4, generally were not the "exact" moments when the transitions occurred. For example, when a wear-rate transition was observed at 33 m, it would mean that the transition actually occurred to the composite somewhere between 16.5 and 33 m.

At the conclusion of the test (66 m), under 1.0 MPa, composite TM had the largest wear-rate value, while composite E had the smallest value; under 1.7 MPa, composite A had the largest wear rate, while composite TM had the smallest wear rate; under 2.4 MPa, composite A had the largest wear rate, while composite E had the smallest wear rate. SEM showed that, under higher loads (1.7 and 2.4 MPa), the surface of composite A suffered more serious damage than the other two composites under the same loads. The lower strength of composite A, as shown in Table I, was believed to have contributed to causing the rapid formation of powdery debris, which, in turn, resulted in higher weight loss.

The slide-induced temperature rises also exhibited transitions. Compared to the friction coefficient data (Fig. 2), it was found that the moments when the transitions in friction occurred were exactly the same as when the transitions in temperature occurred. Because for all three composites the transitions in friction coefficient and in temperature occurred in the same period of sliding distance, it seems reasonable to assume that the transitions in wear took place at the same time.

As shown in Section 3, the type I morphology, which was characterized as a thin, smooth, and bright (under the light microscope) debris film, was accompanied by a low friction coefficient, low wear rate and low temperature. After sliding for some time, the lubricative type I film obviously was no longer mechanically stable and was suddenly disrupted, i.e. the occurrence of transition from type I to type II morphology. The formation of the thick, rough, and dark (under the light microscope) type II powdery debris layer and its effect on wear has been discussed earlier [4–7]. The friction coefficient, wear rate and temperature all increased sharply when the type II debris was formed. Under what conditions the initially formed thin lubricative film became mechanically unstable and exactly how the transition occurred (the mechanism of the film disruption), are not fully established at present. When the composites with a type II debris were slid for a longer distance, in many cases (largely depending on load), the powdery debris was compacted again and formed a smooth, dense and bright (under light microscope) type III debris. When the lubricative type III debris started to develop, the friction coefficient and wear rate both declined, but never approached their initial type I levels.

As mentioned in Section 3, all three composites slid under 1.0 MPa had similar trend in wear-rate variation with slide distance. Their wear rates all decreased initially before 16.5 m. This initial drop in wear rate might be explained by the fact that, in the pre-transitional period, the smooth type I debris film spread over a larger surface with time. In this period, a higher load could also help the type I film to develop. As shown in Fig. 2, in the pre-transitional period, the friction coefficients of composites TM and A slid under 1.7 MPa were each lower than those under 1.0 MPa. As mentioned in Section 1, a decrease in friction with increasing load was also reported for bulk carbon/graphite sliding against self materials and metals, and for carbon fibre-reinforced

polymer matrix composites sliding against metals [11–14].

Table II indicates that, for all composites, a higher load can accelerate the transition from type I to type II, but impedes somewhat the transition from type II to type III. Under 1.0 MPa, all three composites performed similarly. The type III debris was developed before 66 m in all composites. Under 1.7 MPa, the type III debris was observed in composite TM at 66 m. A type II–type III mixed morphology was observed in E. In composite A, type II was not observed to transform into type III. Under 2.4 MPa, type II morphology was never observed to transform into type III morphology throughout the tests in this study.

5. Conclusions

1. In the early stage, all composites slid under a load of 1.0 MPa exhibited low friction coefficients (0.1–0.2). After transition, the friction coefficients rose abruptly to 0.4–0.5, depending on the composite, and then decreased with time to steady values. Under 1.7 MPa, the transition occurred to composites E in the very beginning. The post-transitional friction coefficient of composite A maintained a high level of 0.7–0.9. Under 2.4 MPa, the transition again occurred in the very beginning to composites E and TM. For composite A, the transition occurred much earlier (at about 6 m) than that under 1.7 or 1.0 MPa. The moments when the transitions in friction occurred are exactly the same as when the transitions in temperature occurred.

2. Wear-rate variation with slide distance depended on load and the type of composite. At the conclusion of the test (66 m), under 1.0 MPa, composite TM had the largest wear-rate value, while composite E had the smallest value; under 1.7 MPa, composite A had the largest wear rate, while composite TM had the smallest wear rate; under 2.4 MPa, composite A had the largest wear rate, while composite E had the smallest wear rate.

3. Worn surface morphology was categorized into three types (I, II and III). The friction coefficient, wear rate and temperature all increased sharply when the transition from type I to type II occurred. When the powdery type II debris was compacted to form the lubricative type III debris, the friction coefficient and wear rate declined, but never approached their initial type I levels.

4. For all composites, a higher load can accelerate the transition from type I to type II, but impedes the transition from type II to type III. Under 1.0 MPa, all three composites performed similarly. The type III debris was developed in all composites before 66 m. Under 1.7 MPa, the type III debris was observed in composite TM at 66 m. A type II–type III mixed morphology was observed in E. In composite A, type II was not observed to transform into type III. Under 2.4 MPa, type II morphology was never observed to transform into type III morphology throughout this study.

Acknowledgements

The authors thank the Chung Shan Institute of Science and Technology and the National Science Council of Taiwan, for support of this research under contract CS81-0210-D006-510.

References

1. J. P. RUPPE, *Canad. Aeronaut. Space J.* **26** (1980) 209.
2. I. L. STIMSON and R. FISHER, *Philos. Trans. R. Soc. Lond.* **A294** (1980) 583.
3. S. AWASTHI and J. L. WOOD, *Adv. Ceram. Mater.* **3** (1988) 449.
4. J. D. CHEN and C. P. JU, *Wear* **174** (1994) 129.
5. C. P. JU, K. J. LEE, H. D. WU and C. I. CHEN, *Carbon* **32** (1994) 971.
6. J. D. CHEN and C. P. JU, *ibid.* (1994) in press.
7. *Idem, Mater. Chem. Phys.* **39** (1994) 174.
8. J. K. LANCASTER, in "Proceedings of the 2nd International Conference on Solid Lubrication", Denver, CO, 15–18 August (American Society of Lubrication Engineers, Park Ridge, IL, 1978) p. 176.
9. R. C. BILL, *ibid.*, p. 268.
10. N. MURDIE, C. P. JU, J. DON and F. A. FORTUNATO, *Carbon* **29** (1991) 335.
11. W. T. CLARK, A. CONNOLLY and W. HIRST, *Br. J. Appl. Phys.* **14** (1963) 20.
12. M. A. TANVIR, in "Friction and Traction", edited by D. Dowson, C. M. Taylor, M. Godet and D. Berthe (Westbury house, Guildford, 1981) p. 341.
13. T. F. J. QUINN, *Bri. J. Appl. Phys.* **14** (1963) 107.
14. R. L. FUSARO, *ASLE Trans.* **26** (1983) 209.
15. S. E. HSU and C. I. CHEN, in "Superalloys, Supercomposites and Superceramics", edited by J. K. Tien and T. Caulfield (Academic Press, San Diego, CA, 1989) p. 721.

Received 10 March
and accepted 23 August 1995